Experimental evidence for kinematical focusing in the inelastic scattering of helium from the NaF(001) surface

G. Benedek,* G. Brusdeylins, and J. P. Toennies
Max-Planck Institut für Strömungsforschung, Böttingerstrasse 4-8, 3400 Göttingen, Federal Republic of Germany
R. B. Doak
Bell Laboratories, Murray Hill, New Jersey 07974.
(Received 8 September 1982)

The kinematical focusing (KF) effect along the dispersion curve of Rayleigh waves has been observed in the inelastic scattering of ^{4}He from a NaF(001) surface. From a direct inspection of the time-of-flight spectra, a number of spikes appearing in the angular distribution are discriminated from bound-state resonances and shown to correspond to KF. We show that, in principle, the dispersion relation of Rayleigh waves can be obtained directly from the position of such singularities, without having to resort to time-of-flight measurements.

I. INTRODUCTION

About ten years ago, Williams and Mason[1,2] proposed that high-resolution angular distributions of atoms scattered from crystal surfaces could provide information on surface phonons. Williams and Mason used subtle arguments for attributing the weak streaks observed around the specular peak in a number of out-of-plane scattering experiments to inelastic scattering from single Rayleigh phonons. There is, however, a general difficulty in the analysis of angular distributions. Since the outgoing beam at a given final angle collects inelastically scattered atoms of different energies, an additional selective mechanism must exist to produce sharp inelastic features in the angular spectra. One such mechanism, called *kinematical focusing* (KF), was proposed in a previous theoretical study.[3] KF takes place for any scattering geometry at which the paraboloid representing the energy-gain—versus—momentum-gain relation ("scan curve") probed in an inelastic experiment for given scattering angles,

$$\frac{\omega_s(\vec{\mathrm{K}})}{\omega_i}=\left[\left[1+\frac{K_p}{K_i}\right]^2+\frac{K_{np}^2}{K_i^2}\right]\left[\frac{\sin\theta_i}{\sin\theta_f}\right]^2-1\ , \tag{1}$$

is tangent to a surface-phonon dispersion surface $\omega=\omega_d(\vec{\mathrm{K}})$ (Fig. 1). Here ω_i and K_i are the energy and parallel momentum of the incident atom ($\hbar=1$); θ_i and θ_f are incident and outgoing angles, respectively, measured with respect to the surface normal. $\vec{\mathrm{K}}$ is the total momentum transferred parallel to the surface and has components K_p and K_{np}, $\vec{\mathrm{K}}=(K_p,K_{np})$, parallel and normal to the plane of incidence, respectively. Thus for a given energy there may be a number of angles θ_i and θ_f satisfying the tangency criterion. At these KF angles an extended section of the dispersion curve is seen by the detector, leading to singularities (rainbow effect). The theoretical analysis shows that these singularities can be attributed to the vanishing of the Jacobian transforming momentum-space coordinates into angular coordinates. For relatively heavy particles (such as Ne) and large θ_f and θ_i, KF occurs at small phonon group velocities, i.e., for phonons close to the critical points at the zone boundaries, where the phonon density is large.[3] This, however, is not a strict requirement for KF to be observed. As shown in Sec. IV, with a suitable choice of the kinematical parameters several different tangency points along the phonon-dispersion curve will exist, producing KF features in the angular scan which can be used to obtain an *envelope of the phonon branch from a single angular scan.* Recently, Avila and Lagos have discussed an extension of the KF mechanism valid for nonplanar scattering which explains Williams's and Mason's data by supplying the missing selective mechanism.[4]

Boato and Cantini[5] performed a careful investigation of the in-plane angular distribution of Ne scattered from LiF(001), finding a rich fine structure among the elastic diffraction maxima. The initial interpretation of these inelastic features in terms of KF yielded frequencies of surface modes in reasonable agreement with the theoretical predictions for Rayleigh and Lucas modes at $\bar{M}$ and $\bar{\Gamma}$ critical points.[6] Subsequently, however, Cantini, Felcher, and Tatarek found a more satisfactory explanation of the fine structure in terms in elastic resonances with surface bound states.[7] Their analysis, based on a bound-state resonance selection rule, led to a rough determination of the surface Rayleigh-wave (RW) dispersion. Cantini and Tatarek have now complet-

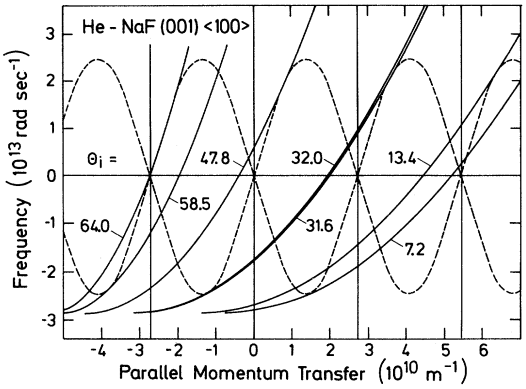

FIG. 1. Scan curves for 90° in-plane scattering of ^{4}He with $k_i=6$ Å^{-1}. The curves shown correspond to incident angles θ_i giving tangency with the Rayleigh-wave dispersion curve (dashed curves). Kinematical focusing occurs for $\theta_f \leq \bar{\theta}_f$ on the annihilation side ($\omega > 0$) and for $\theta_f \geq \bar{\theta}_f$ on the creation side ($\omega < 0$).

ed a similar analysis for the inelastic resonances of He scattered from graphite (0001).[8]

In recent work of Lilienkamp and Toennies[9] and Brusdeylins, Doak, and Toennies,[10–12] the angular distributions for helium scattered from the (001) surfaces of LiF in the ⟨100⟩ azimuth, LiF⟨110⟩, and NaF⟨100⟩, were measured for $k_i \simeq 6$ Å^{-1} and analyzed to elucidate the role of a process called selective desorption.[12] In this process, which was apparently not observed in the analogous experiment by Cantini, Felcher, and Tatarek for $k_i=11$ Å^{-1}, the atoms are first elastically selectively absorbed into one of the bound states with change of parallel momentum corresponding to in-plane and out-of-plane reciprocal-lattice vectors. For LiF⟨100⟩ and NaF⟨100⟩, maxima were found for the in-plane resonances and minima for the out-of-plane resonances. For LiF⟨110⟩ only maxima for the in-plane resonances could be uniquely identified. Since then it has been possible to increase the detection sensitivity to show that for the ⟨110⟩ direction both in-plane and out-of-plane resonances lead to maxima.[9] In this more recent study of phonon-assisted selective desorption and adsorption, where θ_f could be varied independently of θ_i, there is also some evidence for kinematic focusing in the angular distributions, which, however, have not yet been substantiated with the help of time-of-flight (TOF) spectra.

These various investigations of angular distributions have raised some questions concerning the effectiveness of KF, particularly for highly corrugated surfaces, where many strongly coupled bound-state channels lead to resonances which enhance the inelastic scattering and largely mask the KF mechanism. In the present paper we report on a more careful analysis of the angular distributions for He-NaF⟨100⟩, interpreting them in conjunction with time-of-flight spectra. With the time-of-flight spectra some of the angular peaks can now be unambiguously identified as KF.

II. KINEMATICAL FOCUSING EFFECT

For a better understanding of the experimental analysis we briefly recall the mechanism of KF, restricting ourselves to the case of planar scattering.[3] The inelastic part of the scattering angular distribution is obtained by integrating the differential reflection coefficient along the scan curve $\omega=\omega_s(K)$, representing the energy-gain—versus—momentum-gain relation [Eq. (1)]:

$$\frac{dR}{d\Omega}=\int_{\omega=\omega_s(K)} d\omega \frac{d^2R}{d\omega\, d\Omega} , \tag{2}$$

where $d\Omega$ is the solid angle accepted by the detector. For one-phonon processes involving only surface phonons, we write

$$\frac{dR}{d\Omega}=\int_{\omega=\omega_s(K)} dK \frac{\partial \omega_s}{\partial K} A(K)\delta(\omega_s(K)-\omega_d(K)) , \tag{3}$$

where $A(K)$ contains all the information on the dynamic coupling of the atoms to single Rayleigh phonons and is a smooth function of K. Next we assume that for a particular value $\theta_f=\bar{\theta}_f$ the scan curve is tangent to the disperion curve at the point $(\bar{K},\bar{\omega}_d)$. Let us expand around $\bar{K}$ the functions $\omega_d(K)$ and $\omega_s(K)$, the latter for any value of θ_f close to $\bar{\theta}_f$:

$$\omega_d(K)\cong\bar{\omega}_d+(K-\bar{K})\bar{v}_d+\tfrac{1}{2}(K-\bar{K})^2\bar{w}_d , \tag{4}$$

$$\omega_s(K)\cong\omega_s(\bar{K})+(K-\bar{K})\bar{v}_d+\tfrac{1}{2}(K-\bar{K})^2\bar{w} . \tag{5}$$

For either $\theta_f>\bar{\theta}_f$ or $\theta_f<\bar{\theta}_f$ the two intersections between the dispersion and the scan curve are given by

$$K_\pm=\bar{K}\mp\left[2\frac{\omega_s(\bar{K})-\bar{\omega}_d}{\bar{w}_d-\bar{w}}\right]^{1/2} . \tag{6}$$

With this expression and the well-known property of δ functions, we can rewrite the δ function in Eq. (3):

$$\delta(\omega_s(K)-\omega_d(K))=\frac{\delta(K-K_+)+\delta(K-K_-)}{|\,2(\bar{w}_d-\bar{w})[\omega_s(K)-\bar{\omega}_d]\,|^{1/2}} . \tag{7}$$

We now have to expand $\omega_s(K)$ with respect to $\theta_f-\bar{\theta}_f$. In the particular scattering configuration used in the present experiments, θ_f and θ_i are both

variable with the constraint $\theta_i+\theta_f=90°$. For this special case we find

$$\omega_s(\bar{K})\cong\bar{\omega}_d+2\omega_f(1+k_i/k_f)(\bar{\theta}_f-\theta_f)\cot\theta_f\ , \tag{8}$$

where ω_f is the final energy, and k_i and k_f are the incident and final momenta, respectively. By performing the integration in Eq. (3) with the aid of (7) and (8), we obtain

$$\frac{dR}{d\Omega}=\frac{\bar{v}_d A(K)\tan^{1/2}\theta_f}{[\omega_f(1+k_i/k_f)(\bar{w}_d-\bar{w})(\bar{\theta}_f-\theta_f)]^{1/2}}\ . \tag{9}$$

This expression exhibits the inverse square-root singularity at θ_f which characterizes the KF effect. The factor which is more crucial for the KF intensity is $\bar{w}_d-\bar{w}$. When the dispersion and scan curves have about the same curvature at the contact point, the KF has a particularly large effect on the angular distribution. Note that for $\bar{w}_d>\bar{w}$ the peak exists for $\theta_f<\bar{\theta}_f$, and vice versa, so that the square root in Eq. (9) is always real. For the scattering configuration where θ_f is varied and θ_i is kept constant the Jacobian factor $1+k_i/k_f$ in Eq. (9) reduces to 1.[3]

III. EXPERIMENTAL RESULTS

Figure 2 shows the angular distribution of ^{4}He atoms scattered from a NaF(001) surface in the ⟨100⟩ azimuth measured with the same apparatus

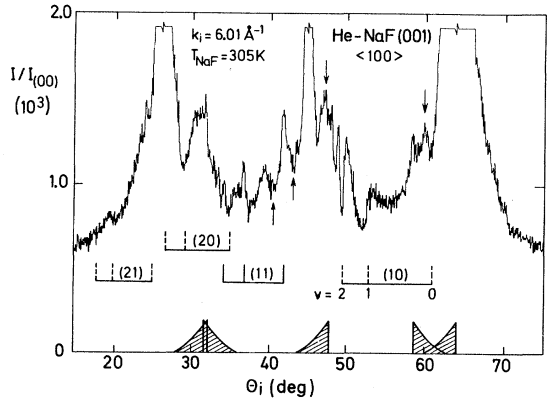

FIG. 2. Angular distribution of He scattered from NaF(001) along the ⟨100⟩ azimuth recorded with high gain to display the minute inelastic features. Values of incident angle at which elastic resonances via $\vec{N}=(1,1)$, (1,0), (2,0), and (2,1) are expected, have been marked for the bound state $v=0,1,2,3$. Phonon-assisted resonances are marked by arrows. The approximate locations and expected peak shapes of kinematical focusing are indicated by the shaded wedges at the bottom of the figure.

and procedure discussed previously.[10,11] The wave vector of the incident atoms was $k_i=6.01$ Å^{-1}+0.4%. The crystal-surface temperature T_s was 300 K for the angular scan in Fig. 2; other spectra with T_s ranging from 136 to 520 K have been measured in order to detect possible temperature effects on the KF.

In addition to specular and diffraction peaks, there are many sharp maxima and minima modulating the inelastic background, which have the following explanations:

(i) Elastic entrance into a bound state. At well-defined incident angles, the incident atoms can enter a bound state elastically by exchanging a surface reciprocal-lattice vector $\vec{N}$ and then leave the surface with the aid of a phonon of momentum $\vec{Q}$ (selective desorption). In Fig. 2 these resonances are indicated by brackets. The predicted in-plane resonances for $\vec{N}=(1,1)$ correspond to maxima, whereas out-of-plane resonances $[\vec{N}=(1,0),(2,0),(2,1)]$ coincide with the observed minima.

(ii) Phonon-assisted entrance into a bound state. A number of incident atoms scatter into a bound state with the aid of a vector $\vec{N}$ and of a phonon of momentum $\vec{Q}$. In the specific case of NaF (Fig. 2) the maxima at 59.8° and 47.1° (downward arrows) are found to be associated with the same sharp $(1,1)_{v=0}$ resonance via a Rayleigh-phonon—creation and —annihilation process, respectively. The minima at 40.3° and 42.8° (upward arrows) correspond to the out-of-plane resonances $(1,0)_1$ and $(1,0)_2$ assisted by a Rayleigh-phonon—creation process. For phonon-assisted resonances, only the scattered intensity for that specific phonon is sharply enhanced or depressed, so that the TOF spectra for θ_i varying across an inelastic resonance are affected by strong localized distortions.

(iii) Kinematical focusing. Owing to the inverse-square-root singularity, Eq. (9), asymmetric maxima—rising smoothly on one side and abruptly on the other—will appear in the angular distribution. When θ_f approaches $\bar{\theta}_f$ from the smooth side, two surface-phonon peaks in the TOF spectrum move closer and closer and disappear abruptly as θ_f goes beyond $\bar{\theta}_f$, on the sharp side. Since this sudden modification takes place within a few tenths of a degree, the remaining part of the TOF spectrum remains practically unchanged.

The three pairs of TOF spectra for $\theta_i=32.0°$ and 32.5° (Fig. 3), $\theta_i=48°$ and 49° (Fig. 4), and $\theta_i=64.2°$ and 64.5° (Fig. 5) offer clear evidence of this effect. Particularly for $\theta_i=64.2°$ the two close RW peaks seen at $\sim$1.9 msec disappear for a change of θ_i as small as +0.3°. Therefore the three sharp peaks found in the angular distribution at $\theta_i=32.0°$, 48.0°, and 64.3° (the latter is out of scale in Fig. 1) are as-

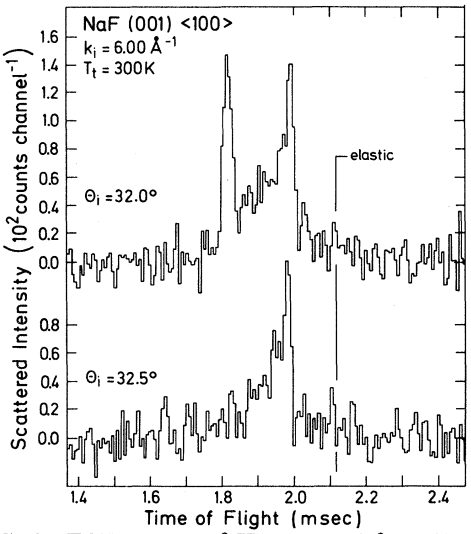

FIG. 3. TOF spectra of He scattered from NaF(001) along the ⟨100⟩ azimuth for $\theta_i = 32.0°$ and 32.5°, illustrating the KF effect occurring at 32°.

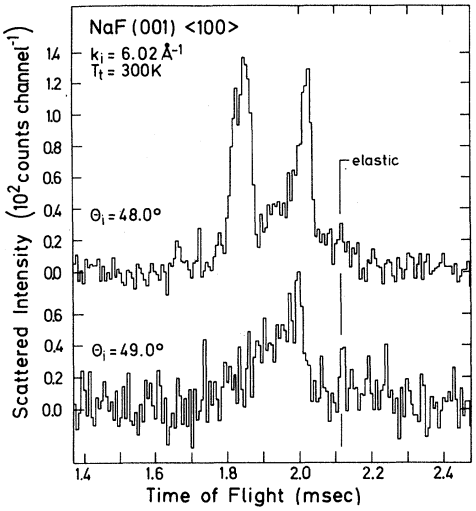

FIG. 4. TOF spectra of He scattered from NaF(001) along the ⟨100⟩ azimuth for $\theta_i = 48.0°$ and 49.0°, illustrating the KF effect occurring at 48°.

cribed to the KF effect involving annihilation of Rayleigh phonons. Two other features at $\theta_i = 30.5°$ and 58.2°, which become more evident at low temperature, are tentatively attributed to KF with creation of Rayleigh phonons. Here confirmation with TOF spectra was not possible, however, since the signal-to-noise ratio for slow atoms (creation of highly energetic phonons) is too unfavorable.

Once the KF angles are identified in the angular distribution, one can readily obtain an envelope of the RW dispersion curve just by folding the corresponding scan curves into the irreducible part of the first Brillouin zone for positive frequencies (Fig. 6). In the resulting diagram we have added the straight line $\omega = v_R K$, valid in the continuum limit ($v_R = 3120$ m/sec),[13] and a selection of the experimental points obtained from TOF spectra.

It is interesting to note that the error bar for the KF scan curves may be smaller than the spread of the experimental points deduced from peaks in TOF spectra. This is due to the fact that KF peaks depend only on the uncertainties in θ_i but not directly on the time-of-flight resolution.

IV. DISCUSSION

The relatively precise determination of the RW dispersion relation from the envelope of the tangent scan curves illustrates the practical importance of the KF effect. In principle one can obtain a preliminary knowledge of the surface-phonon dispersion from a single high-resolution angular distribution before resorting to the measurement of TOF spectra. In practice, it is hard to recognize KF peaks among the large number of resonant features without examining TOF spectra. Other ways of identification, however, can be suggested. One is based on the rather general behavior of resonance under an azimuthal rotation ϕ of the scattering place away from a symmetry direction. In-plane resonances yielding maxima for $\phi = 0$ gradually decrease as ϕ is

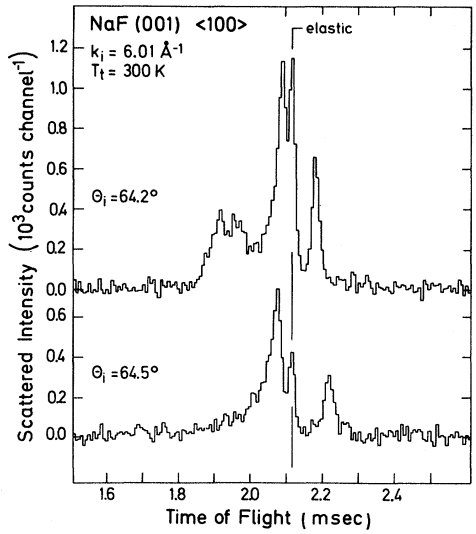

FIG. 5. TOF spectra of He scattered from NaF(001) along the ⟨100⟩ azimuth for $\theta_i = 64.2°$ and 64.5°, illustrating the KF effect occurring at 64.3°.

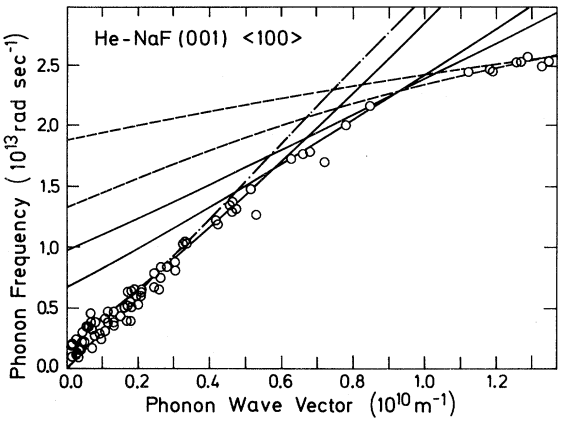

FIG. 6. Scan curves corresponding to the KF angles for phonon annihilation (continuous lines) and creation (broken lines) have been folded into the irreducible part of the surface Brillouin zone for positive frequency. The long-wavelength Rayleigh velocity (dashed-dotted line) is also shown. The resulting envelope of the RW dispersion curve compares well with experimental points derived from TOF spectra.

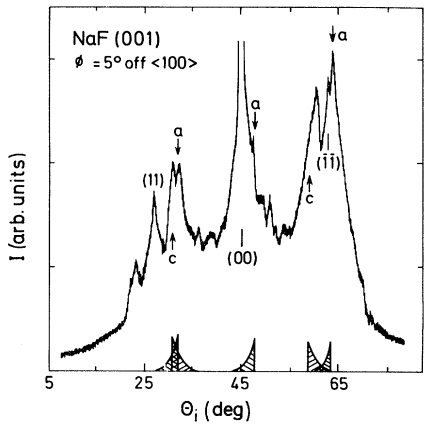

FIG. 7. Angular distribution of He scattered from NaF(001) at an azimuth $\phi = 5°$ slightly removed from the $\langle 100 \rangle$ direction. Incident angles corresponding to KF by annihilation (a) and creation (c) of phonons are indicated. Such off-symmetry distributions may allow the KF features to be unambiguously identified without TOF.

changed, whereas KF peaks remain fairly constant. This is illustrated in Fig. 7 for helium scattered from NaF(001) at an incident azimuth 5° removed from the $\langle 100 \rangle$ direction.[14] In this direction the (11) and $(\bar{1}1)$ diffraction peaks are no longer to be seen apart from remnants due to diffuse elastic or low-frequency inelastic scattering. Nevertheless, strong features remain in the angular distribution at incident polar angles corresponding to kinematical focusing (although TOF spectra have not yet been taken to verify these assignments). Similar behavior has been observed in scattering from NaCl(001).[15] Finally we point out that beyond some angle ϕ the KF effect may disappear altogether. This was inferred from a time-of-flight study of LiF where the inelastic peaks near the (11) diffraction peak were seen to coalesce with increasing ϕ and were expected to disappear for $\phi > 8°$.[11] The temperature dependence of KF peaks may also be useful in discriminating them from resonances. In fact, a difference between the temperature dependence of KF and resonance processes, essentially through the Debye-Waller factor, can be argued.

Of course the KF effect could be better exploited in surfaces with a small corrugation, where bound-state resonances are negligible, as, for instance, in metals. We do not yet know of any such example except possibly a few poorly understood data on Au(111)-He reported by Miller and Horne.[16] We remark finally that kinematical focusing can in principle occur also with the bulk modes at the lower edge of the longitudinal-acoustic (LA) band. Along the LA edge the surface-projected phonon density shows a peak whose intensity in some case is comparable to that of the RW.[17] In this case KF could also possibly provide information on LA bulk modes along a symmetry direction.

ACKNOWLEDGMENTS

We thank R. Rechsteiner and J. Skofronick for carrying out the measurements shown in Fig. 7. One of us (G.B.) is grateful for the kind hospitality enjoyed at the Max-Planck-Institut für Strömungsforschung, Göttingen. One of us (R.B.D.) thanks the Deutscher Akademischer Austauschdienst for a stipend during the course of much of this work.

*Permanent address: Gruppo Nazionale di Struttura della Materia del Consiglio Nazionale delle Ricerche, Istituto di Fisica dell'Universita, Via Celoria 16, 20133 Milano, Italy

[1]B. R. Williams, J. Chem. Phys. 55, 1315 (1971); 55, 3220 (1971).

[2]B. F. Mason and B. R. Williams, J. Chem. Phys. 61, 2765 (1974).

[3]G. Benedek, Phys. Rev. Lett. 35, 234 (1975).

[4]R. Avila and M. Lagos, Surf. Sci. 103, L104 (1981).

[5]G. Boato and P. Cantini, in *Dynamical Processes at Crystal Surfaces, Proceedings of the International School of*

Physics, "Enrico Fermi," Course LVIII, 1973, edited by F. O. Goodman (Compositori, Bologna, 1974), p. 707, and private communication.

[6]T. S. Chen, F. W. de Wette, and G. P. Alldredge, Phys. Rev. B 15, 1167 (1977). See particularly Refs. 41 and 42 within.

[7]P. Cantini, G. P. Felcher, and R. Tatarek, Phys. Rev. Lett. 37, 606 (1976).

[8]P. Cantini and R. Tatarek, Surf. Sci. 114, 471 (1982).

[9]G. Lilienkamp and J. P. Toennies (unpublished).

[10]G. Brusdeylins, R. B. Doak, and J. P. Toennies, Phys. Rev. Lett. 44, 1417 (1980); 46, 437 (1981).

[11]G. Brusdeylins, R. B. Doak, and J. P. Toennies (unpublished); R. B. Doak, Ph.D. thesis, Massachusetts Institute of Technology, 1981 (Max-Planck-Institut für Strömungsforschung, Göttingen, Bericht 14/1981).

[12]G. Brusdeylins, R. B. Doak, and J. P. Toennies, J. Chem. Phys. 75, 1784 (1981).

[13]G. W. Farnell, *Physical Acoustics* (Academic, New York, 1970), Vol. VI, p. 109.

[14]G. Brusdeylins, R. Rechsteiner, and J. G. Skofronick (unpublished).

[15]G. Benedek, G. Brusdeylins, R. B. Doak, J. G. Skofronick, and J. P. Toennies (unpublished).

[16]D. R. Miller and J. M. Horne, in *Proceedings of the 7th International Vacuum Congress and 3rd International Conference on Solid Surfaces,* edited by R. Dobrozemsky, F. Rüdenauer, F. P. Viehbock, and A. Breth (Berger, Vienna, 1977), p. 1385.

[17]G. Benedek, R. B. Doak, and J. P. Toennies (unpublished).